Hydrodynamic coupling of two rotating spheres trapped in harmonic potentials

Michael Reichert* and Holger Stark

Fachbereich Physik, Universität Konstanz, D-78457 Konstanz, Germany
(Received 11 July 2003; revised manuscript received 14 October 2003; published 30 March 2004)

We theoretically study in detail the hydrodynamic coupling of two equal-sized colloidal spheres at low Reynolds numbers assuming the particles to be harmonically trapped with respect to both their positions and orientations. By taking into account the rotational motion, we obtain a rich spectrum of collective eigenmodes whose properties we determine on the basis of pure symmetry arguments. Extending recent investigations on translational correlations [J.-C. Meiners and S. R. Quake, Phys. Rev. Lett. **82**, 2211 (1999)], we derive the complete set of autocorrelation and cross-correlation functions emphasizing the coupling of rotation to translation which we illustrate in a few examples. An important feature of our system is the self-coupling of translation and rotation of one particle mediated by the neighboring particle that is clearly visible in the appropriate autocorrelation function. This coupling is a higher-order effect and therefore not included in the widely used Rotne-Prager approximation for the hydrodynamic mobilities.

I. INTRODUCTION

Colloids are widely used to model atomic systems [1,2]. However, there is one feature specific to colloidal suspensions which distinguishes them fundamentally from atomic systems: the so-called hydrodynamic interactions [3,4]. A particle moving in a viscous fluid creates a long-range flow field around itself through which it interacts with other particles. Thus, hydrodynamic interactions constitute a complicated many-body problem since the motion of one particle depends on the translations and rotations of all the other particles in the fluid [5].

The central quantities in the description of hydrodynamic interactions are the mobility or friction tensors which connect in a linear response scheme all the forces and torques acting on the particles to their linear and angular velocities [6]. In the present paper, we draw special attention to the rotational degree of freedom and how it couples to translation. Its physical consequences have rarely been treated in literature [7–9].

In many physically interesting systems, hydrodynamic interactions play an important role. Whenever dynamic effects in suspensions are studied, hydrodynamic interactions have to be taken into account. Examples are sedimenting particles [10,11] or the apparent attractive interaction between like-charged spherical particles mediated by a single, like-charged wall [12].

In recent years, a new method called microrheology has been developed [13] and applied to several biological systems [14,15]. It is used to determine rheological properties of viscous and viscoelastic media by tracking the trajectory of embedded probe particles and calculating the time-dependent position correlations. The so-called two-point microrheology employs a system of two colloidal particles, which has several advantages over using only a single particle; in particular, the correlated motions of two tracer particles reflect the bulk rheology of the medium they are embedded in more

accurately [16,17]. Many experiments based on this technique have been carried out to study soft media [18–21]. Furthermore, this method was used to measure the corrections to the diffusion coefficients in a system of two spheres due to hydrodynamic interactions [22] and to study the hydrodynamic coupling of two spheres to a wall [23].

The physical systems we have in mind are colloidal suspensions of birefringent spherical particles. For example, they are realized by polymerizing the nematic order in liquid-crystal droplets [24,25]. In contrast to conventional isotropic colloids, both their positions and orientations can be manipulated by optical tweezers. In particular, the orientation is controlled with optical traps generated by linearly polarized laser light and is detected, e.g., with crossed polarizers [24–26] (see Fig. 1).

In the present paper, we consider a system of two trapped spheres of equal size. We give a complete analytic description of the coupled translational and rotational dynamics. Due to the axial symmetry, the longitudinal motions parallel to the particle-particle axis decouple completely from transversal motions. In addition, there is no coupling of translation and rotation in longitudinal motions. This greatly reduces the complexity of the problem. We determine the
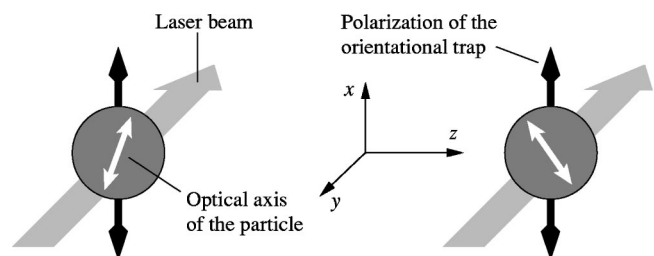

FIG. 1. Sketch of a setup to monitor rotational correlations of two birefringent particles. The particles are situated on the *z* axis. The laser beam of the orientational optical trap is directed along the *y* axis and its polarization points into *x* direction. To monitor transversal correlations, the direction of observation is along the *y* axis. Pure longitudinal rotational correlations are only observable along the *z* axis.

*Electronic address: michael.reichert@uni-konstanz.de

complete set of collective eigenmodes of the system and calculate the correlations for particles undergoing thermal fluctuations. Our work extends recent investigations on correlations in translational fluctuations [18–20]. By taking into account the rotational degrees of freedom, we obtain a rich spectrum of collective modes and correlation functions.

The outline of this paper is as follows. In Sec. II, we first summarize the basic equations for the description of hydrodynamic interactions in general. Then, we study in detail the two-particle system and show by symmetry arguments how it decouples into the aforementioned longitudinal and transversal motions. Assuming that both the particles' positions and orientations are trapped in harmonic potentials, we determine and discuss their collective eigenmodes in Sec. III. Finally, in Sec. IV, we use Langevin dynamics to calculate correlation functions for the thermally fluctuating positions and orientations of the trapped particles and point out their interesting features.

II. HYDRODYNAMIC INTERACTIONS

A. Fundamental equations

In the regime of low Reynolds numbers and on the Brownian time scale, the flow of an incompressible fluid with viscosity η obeys the Stokes or creeping flow equations [3]

$$\eta \nabla^2 \boldsymbol{u} - \boldsymbol{\nabla} p = \boldsymbol{0}, \quad \boldsymbol{\nabla} \cdot \boldsymbol{u} = 0, \tag{1}$$

where $\boldsymbol{u}$ is the flow field and p the hydrodynamic pressure. Stokesian dynamics describes overdamped motion in a viscous fluid. In the following, we consider motions of particles in an unbounded and otherwise quiescent fluid, i.e., $\boldsymbol{u} = \boldsymbol{0}$ at infinity.

Imposing stick boundary conditions on the surfaces of all N particles suspended in the fluid at positions $\boldsymbol{r}_i$ ($i = 1, \ldots, N$), the motions of the particles are mutually coupled via the flow field. Due to the linearity of Eqs. (1), the translational and rotational velocities of the particles, $\boldsymbol{v}_i$ and $\boldsymbol{\omega}_i$, depend linearly on all external forces and torques acting on the particles, $\boldsymbol{F}_j$ and $\boldsymbol{T}_j$ [6]:

$$\boldsymbol{v}_i = \sum_{j=1}^{N} (\boldsymbol{\mu}_{ij}^{\mathrm{tt}} \boldsymbol{F}_j + \boldsymbol{\mu}_{ij}^{\mathrm{tr}} \boldsymbol{T}_j), \tag{2a}$$

$$\boldsymbol{\omega}_i = \sum_{j=1}^{N} (\boldsymbol{\mu}_{ij}^{\mathrm{rt}} \boldsymbol{F}_j + \boldsymbol{\mu}_{ij}^{\mathrm{rr}} \boldsymbol{T}_j). \tag{2b}$$

The central quantities constituting the mutual coupling of translation and rotation (denoted by superscripts t and r) of two particles i and j are the 3×3 mobility tensors $\boldsymbol{\mu}_{ij}^{\mathrm{tt}}$, $\boldsymbol{\mu}_{ij}^{\mathrm{rr}}$, $\boldsymbol{\mu}_{ij}^{\mathrm{tr}}$, and $\boldsymbol{\mu}_{ij}^{\mathrm{rt}}$. They depend on the current spatial configuration of all particles, i.e., the set of position vectors $\{\boldsymbol{r}_1, \ldots, \boldsymbol{r}_N\}$ in the case of spherical particles.

To introduce a more compact notation, we define the $6N$-dimensional vectors $\mathbf{V} = [\boldsymbol{v}_1, \ldots, \boldsymbol{v}_N, \boldsymbol{\omega}_1, \ldots, \boldsymbol{\omega}_N]$ and $\mathbf{F} = [\boldsymbol{F}_1, \ldots, \boldsymbol{F}_N, \boldsymbol{T}_1, \ldots, \boldsymbol{T}_N]$. Then, Eqs. (2) take the form

$$\mathbf{V} = \mathbf{M} \mathbf{F} \tag{3}$$

with the $6N \times 6N$ mobility matrix

$$\mathbf{M} = \begin{bmatrix} [\boldsymbol{\mu}_{ij}^{\mathrm{tt}}] & [\boldsymbol{\mu}_{ij}^{\mathrm{tr}}] \\ [\boldsymbol{\mu}_{ij}^{\mathrm{rt}}] & [\boldsymbol{\mu}_{ij}^{\mathrm{rr}}] \end{bmatrix}, \tag{4}$$

where the four blocks of $\mathbf{M}$ consist each of $N \times N$ matrices whose elements are the 3×3 mobility tensors; e.g.,

$$[\boldsymbol{\mu}_{ij}^{\mathrm{tt}}] = \begin{bmatrix} \boldsymbol{\mu}_{11}^{\mathrm{tt}} & \cdots & \boldsymbol{\mu}_{1N}^{\mathrm{tt}} \\ \vdots & \ddots & \vdots \\ \boldsymbol{\mu}_{N1}^{\mathrm{tt}} & \cdots & \boldsymbol{\mu}_{NN}^{\mathrm{tt}} \end{bmatrix}. \tag{5}$$

According to the reciprocal theorem of Lorentz, the mobility tensors fulfill the symmetry relations [6]

$$(\boldsymbol{\mu}_{ij}^{\mathrm{tt}})^{\mathrm{T}} = \boldsymbol{\mu}_{ji}^{\mathrm{tt}}, \quad (\boldsymbol{\mu}_{ij}^{\mathrm{rr}})^{\mathrm{T}} = \boldsymbol{\mu}_{ji}^{\mathrm{rr}}, \quad (\boldsymbol{\mu}_{ij}^{\mathrm{tr}})^{\mathrm{T}} = \boldsymbol{\mu}_{ji}^{\mathrm{rt}}, \tag{6}$$

where $(\boldsymbol{\mu}_{ij}^{\mathrm{tt}})^{\mathrm{T}}$ denotes the transpose of $\boldsymbol{\mu}_{ij}^{\mathrm{tt}}$, etc. Thus, the entire $6N \times 6N$ matrix $\mathbf{M}$ is symmetric.

In the overdamped limit discussed here, the work done on the particles by the external forces and torques $\mathbf{F}$ is completely dissipated in the fluid, so the energy dissipation rate $\Sigma_i (\boldsymbol{v}_i \cdot \boldsymbol{F}_i + \boldsymbol{\omega}_i \cdot \boldsymbol{T}_i) = \mathbf{V} \cdot \mathbf{F} = \mathbf{V} \cdot \mathbf{M}^{-1} \mathbf{V}$ has to be positive. Therefore, the friction matrix $\mathbf{M}^{-1}$ and hence the mobility matrix $\mathbf{M}$ itself are positive definite.

There are several methods to calculate the mobility tensors for a given many-particle system, e.g., the concept of reflected flow fields using the gradient expansion technique [3,6] or the method of induced force multipoles [5,27]. The latter was implemented in the numerical library HYDROLIB [28] which calculates the mobility or friction matrix for a given configuration of spheres.

B. Two-sphere system

In the following, we consider a system of two equal-sized spheres. Let $\boldsymbol{r}$ be the vector connecting the centers of the two spheres, pointing from sphere 1 to sphere 2, and r the center-to-center distance. Then, $\hat{\boldsymbol{r}} = \boldsymbol{r}/r$ is the unit vector along the line of centers. Due to the rotational symmetry about the axis $\hat{\boldsymbol{r}}$ and the different parities of polar ($\boldsymbol{v}_i$ and $\boldsymbol{F}_i$) and pseudo-vectors ($\boldsymbol{\omega}_i$ and $\boldsymbol{T}_i$), the mobility tensors can be written as [29]

$$\boldsymbol{\mu}_{ij}^{\mathrm{tt}}(\boldsymbol{r}) = \mu_{ij}^{\mathrm{tt}\|}(r) \hat{\boldsymbol{r}} \otimes \hat{\boldsymbol{r}} + \mu_{ij}^{\mathrm{tt}\perp}(r)(\mathbf{1} - \hat{\boldsymbol{r}} \otimes \hat{\boldsymbol{r}}), \tag{7a}$$

$$\boldsymbol{\mu}_{ij}^{\mathrm{rr}}(\boldsymbol{r}) = \mu_{ij}^{\mathrm{rr}\|}(r) \hat{\boldsymbol{r}} \otimes \hat{\boldsymbol{r}} + \mu_{ij}^{\mathrm{rr}\perp}(r)(\mathbf{1} - \hat{\boldsymbol{r}} \otimes \hat{\boldsymbol{r}}), \tag{7b}$$

$$\boldsymbol{\mu}_{ij}^{\mathrm{tr}}(\boldsymbol{r}) = \mu_{ij}^{\mathrm{tr}\perp}(r) \hat{\boldsymbol{r}} \times. \tag{7c}$$

The mobility coefficients $\mu_{ij}^{\mathrm{tt}\|,\perp}$, $\mu_{ij}^{\mathrm{rr}\|,\perp}$, and $\mu_{ij}^{\mathrm{tr}\perp}$ ($i,j = 1,2$) are scalar functions depending only on the center-to-center distance r. They describe motions parallel and perpendicular to the axis, respectively. Using the general symmetry relations (6) and the fact that particles 1 and 2 are identical, the mobility coefficients obey [29]

$$\mu_{11}^{\mathrm{tt}\|,\perp} = \mu_{22}^{\mathrm{tt}\|,\perp}, \quad \mu_{11}^{\mathrm{rr}\|,\perp} = \mu_{22}^{\mathrm{rr}\|,\perp}, \quad \mu_{11}^{\mathrm{tr}\perp} = -\mu_{22}^{\mathrm{tr}\perp}, \tag{8a}$$
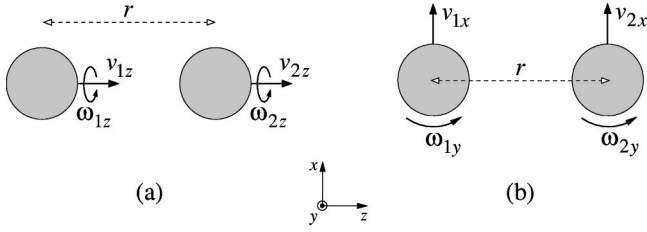
FIG. 2. Definition of the applied Cartesian coordinate system. The z direction is along the center-to-center line of the two spheres. Longitudinal motions (a) decouple from transversal motions (b). Furthermore, there is no coupling of translation and rotation for longitudinal motions.

$$\mu_{12}^{tt\|,\perp} = \mu_{21}^{tt\|,\perp}, \quad \mu_{12}^{rr\|,\perp} = \mu_{21}^{rr\|,\perp}, \quad \mu_{12}^{tr\perp} = -\mu_{21}^{tr\perp}. \quad (8b)$$

With the explicit expressions (7), the dynamics of the two-sphere system described by Eq. (3) separates into longitudinal motions parallel and transversal motions perpendicular to the particle-particle axis $\hat{r}$. Furthermore, longitudinal translations and longitudinal rotations (i.e., rotations about the axis) do not couple to each other because of the different parities of translations (polar vectors) and rotations (axial vectors). In a Cartesian coordinate system with the z direction pointing along $\hat{r}$ (see Fig. 2), we obtain from Eqs. (2), (7), and (8b) for longitudinal motions

$$\begin{bmatrix} v_{1z} \\ v_{2z} \\ \omega_{1z} \\ \omega_{2z} \end{bmatrix} = \begin{bmatrix} \mu_{11}^{tt\|} & \mu_{12}^{tt\|} & 0 & 0 \\ \mu_{12}^{tt\|} & \mu_{11}^{tt\|} & 0 & 0 \\ 0 & 0 & \mu_{11}^{rr\|} & \mu_{12}^{rr\|} \\ 0 & 0 & \mu_{12}^{rr\|} & \mu_{11}^{rr\|} \end{bmatrix} \begin{bmatrix} F_{1z} \\ F_{2z} \\ T_{1z} \\ T_{2z} \end{bmatrix}, \quad (9)$$

where v_{1z} is the z component of the translational velocity of particle 1, etc. In transversal motions, translations along the x direction are coupled to rotations about the y axis:

$$\begin{bmatrix} v_{1x} \\ v_{2x} \\ \omega_{1y} \\ \omega_{2y} \end{bmatrix} = \begin{bmatrix} \mu_{11}^{tt\perp} & \mu_{12}^{tt\perp} & -\mu_{11}^{tr\perp} & -\mu_{12}^{tr\perp} \\ \mu_{12}^{tt\perp} & \mu_{11}^{tt\perp} & \mu_{12}^{tr\perp} & \mu_{11}^{tr\perp} \\ -\mu_{11}^{tr\perp} & \mu_{12}^{tr\perp} & \mu_{11}^{rr\perp} & \mu_{12}^{rr\perp} \\ -\mu_{12}^{tr\perp} & \mu_{11}^{tr\perp} & \mu_{12}^{rr\perp} & \mu_{11}^{rr\perp} \end{bmatrix} \begin{bmatrix} F_{1x} \\ F_{2x} \\ T_{1y} \\ T_{2y} \end{bmatrix}. \quad (10)$$

Translations along the y direction and rotations about the x axis obey an equivalent system of equations.

Defining a four-dimensional velocity vector $\mathbf{v}$ and a force vector $\mathbf{f}$, we abbreviate Eqs. (9) and (10), respectively, by

$$\mathbf{v} = \mathbf{mf}, \quad (11)$$

where the appropriate 4×4 mobility matrix $\mathbf{m}$ is still symmetric. Thus, rotational symmetry reduces the full 12×12 problem (3) to two 4×4 problems, where Eq. (9) is essentially a 2×2 problem.

Accordingly, the energy dissipation rate $\mathbf{V} \cdot \mathbf{M}^{-1} \mathbf{V}$ splits up into a sum of three independent terms of the form $\mathbf{v} \cdot \mathbf{m}^{-1} \mathbf{v}$, so the single-mobility matrices $\mathbf{m}$ have to be positive definite.

C. Mobilities in Rotne-Prager approximation

For a system of two particles, the mobility tensors can be calculated, e.g., with the method of reflections based on the Faxén theorem. It provides a systematic expansion of the mobility tensors in powers of the inverse particle separation (for a detailed description, see, e.g., Ref. [3]).

The leading order in the far-field approximation of the mobilities is the well-known Oseen tensor which considers the particles as pointlike and hence does not include rotations. The next-higher order is the so-called Rotne-Prager approximation. It corresponds to one reflection of the flow field and is therefore exact up to the order of $1/\rho^3$, where $\rho = r/a$ is the dimensionless particle distance (a is the radius of the spheres). The relevant mobilities including the rotational degrees of freedom are presented, e.g., in Refs. [30,29]. They also follow straightforwardly by extending the calculations in Ref. [3], where the torques are explicitly set to zero.

In the Rotne-Prager approximation, the self-mobilities are identical to the Stokes coefficients for single spheres,

$$\boldsymbol{\mu}_{ii}^{tt} = \mu^t \mathbf{1}, \quad \text{where} \quad \mu^t = (6\pi\eta a)^{-1}, \quad (12)$$

$$\boldsymbol{\mu}_{ii}^{rr} = \mu^r \mathbf{1}, \quad \text{where} \quad \mu^r = (8\pi\eta a^3)^{-1}, \quad (13)$$

and there is no self-coupling of translation and rotation, i.e.,

$$\boldsymbol{\mu}_{ii}^{tr} = \boldsymbol{\mu}_{ii}^{rt} = \mathbf{0}. \quad (14)$$

Note that for an isolated sphere within the linear Stokes regime, translation and rotation are not coupled; the so-called Magnus effect only enters via the nonlinear term in the Navier-Stokes equation [31]. On the other hand, in the two-sphere system, the self-coupling exists since it is mediated by the second particle. However, this is an effect of higher order than $1/\rho^3$ and therefore not included in the Rotne-Prager approximation, as stated in Eq. (14).

For completeness, we also give the essential cross mobilities:

$$\boldsymbol{\mu}_{12}^{tt} = \mu^t \left[\frac{3}{4\rho}(\mathbf{1} + \hat{r} \otimes \hat{r}) + \frac{1}{2\rho^3}(\mathbf{1} - 3\hat{r} \otimes \hat{r}) \right], \quad (15)$$

$$\boldsymbol{\mu}_{12}^{rr} = \mu^r \left[-\frac{1}{2\rho^3}(\mathbf{1} - 3\hat{r} \otimes \hat{r}) \right], \quad (16)$$

$$\boldsymbol{\mu}_{12}^{tr} = \mu^r \left[a\frac{1}{\rho^2}\hat{r} \times \right]. \quad (17)$$

III. EIGENMODES OF TWO TRAPPED SPHERES

We aim to study thermal motions of particles that are trapped with respect to both their positions and orientations.
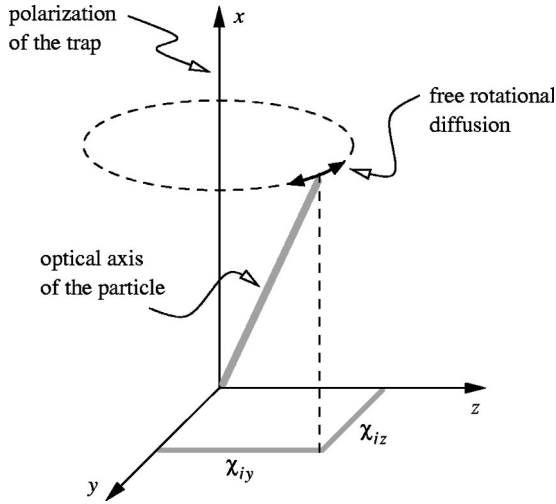
FIG. 3. While the rotation of the optical axis of the trapped particle about the direction of the trap polarization (here pointing along the x axis) is free, the deviation from the x direction is restricted, and therefore the angular displacements χ_{iy} and χ_{iz} are small (see text).

Assuming that the spatial and angular displacements are small, we consider harmonic trap forces and torques, i.e.,

$$F_{i\alpha} = -k^{\mathrm{t}} r_{i\alpha}, \qquad (18)$$

$$T_{i\alpha} = -k^{\mathrm{r}} \chi_{i\alpha}, \qquad (19)$$

where k^{t} and k^{r} are positive force and torque constants ($i = 1,2$ is the particle number and $\alpha = x,y,z$ the coordinate index). The particle velocities are

$$v_{i\alpha} = \dot{r}_{i\alpha}, \qquad (20)$$

where the spatial coordinate $r_{i\alpha}$ denotes the displacement of particle i along direction α.

The angle $\chi_{i\alpha}$ describes the rotation of particle i about the coordinate axis α. As long as this angular displacement is small ($\langle \chi_{i\alpha}^2 \rangle \ll 1$), we can relate it to the angular velocity via

$$\omega_{i\alpha} = \dot{\chi}_{i\alpha}. \qquad (21)$$

This is a nontrivial statement and requires some explanation. The optical axis of the trapped birefringent particle aligns along the polarization of the laser trap pointing along, e.g., the x axis (see Fig. 3). Any deviation of the particle orientation from the x direction is described by the angles χ_{iy} and χ_{iz}, and relaxes in the optical trap on the time scale $(k^{\mathrm{r}} \mu^{\mathrm{r}})^{-1}$. However, the free rotational diffusion of the particle axis about the x direction also changes the angular displacements χ_{iy} and χ_{iz} (see Fig. 3), and therefore, relation (21) does not hold in general. Nevertheless, in the limit considered here the orientational relaxation is a much faster process than the free diffusion, so on the relaxation time scale $(k^{\mathrm{r}} \mu^{\mathrm{r}})^{-1}$, the free diffusion can be neglected and relation (21) is applicable. To show this, we note that the free rotational diffusion takes place on the time scale $(k_{\mathrm{B}} T \mu^{\mathrm{r}})^{-1}$. Requiring that $(k^{\mathrm{r}} \mu^{\mathrm{r}})^{-1}/(k_{\mathrm{B}} T \mu^{\mathrm{r}})^{-1} = k_{\mathrm{B}} T/k^{\mathrm{r}} \ll 1$ and using

the equipartition theorem yields $\langle \chi_{i\alpha}^2 \rangle = k_{\mathrm{B}} T/k^{\mathrm{r}} \ll 1$, which is consistent with the initial assumption.

We define generalized coordinates $\mathbf{q} = [r_{1z}, r_{2z}, \chi_{1z}, \chi_{2z}]$ for longitudinal modes and $\mathbf{q} = [r_{1x}, r_{2x}, \chi_{1y}, \chi_{2y}]$ for transversal modes, and combine the corresponding trap forces (18) and torques (19) into a four-dimensional vector

$$\mathbf{f} = -\mathbf{kq} \qquad (22)$$

with the diagonal force constant matrix

$$\mathbf{k} = \begin{bmatrix} k^{\mathrm{t}} & 0 & 0 & 0 \\ 0 & k^{\mathrm{t}} & 0 & 0 \\ 0 & 0 & k^{\mathrm{r}} & 0 \\ 0 & 0 & 0 & k^{\mathrm{r}} \end{bmatrix}. \qquad (23)$$

Then, the equation of motion (11) for both longitudinal and transversal modes reads

$$\dot{\mathbf{q}} + \mathbf{mkq} = \mathbf{0}, \qquad (24)$$

where $\mathbf{m}$ is the appropriate mobility matrix given by Eqs. (9) and (10), respectively. Note that for spatial displacements small compared to the equilibrium particle distance, we can consider $\mathbf{m}$ to be constant.

The solutions of Eq. (24) are relaxational eigenmodes $e^{-\lambda_n t} \mathbf{a}_n$ with relaxation rates λ_n or relaxation times λ_n^{-1}. They are determined by the eigenvalue problem

$$\mathbf{mka}_n = \lambda_n \mathbf{a}_n \quad (n = 1, \ldots, 4) \qquad (25)$$

of the nonsymmetric 4×4 matrix $\mathbf{mk}$ whose eigenvectors $\mathbf{a}_n$ are in general not perpendicular to each other. In the next two sections, we will analyze the eigenmodes in detail.

A. Longitudinal eigenmodes

To study the longitudinal eigenmodes, the traps have to be polarized along the x or y direction so that the angular displacements χ_{iz} are small. Since longitudinal translations and rotations are decoupled (as discussed in Sec. II B), we can immediately write down the eigenvalues and eigenvectors of the four eigenmodes:

$$\lambda_{1/2} = k^{\mathrm{t}}(\mu_{11}^{\mathrm{tt}\parallel} \pm \mu_{12}^{\mathrm{tt}\parallel}), \quad \mathbf{a}_{1/2} = [1, \pm 1, 0, 0], \qquad (26a)$$

$$\lambda_{3/4} = k^{\mathrm{r}}(\mu_{11}^{\mathrm{rr}\parallel} \pm \mu_{12}^{\mathrm{rr}\parallel}), \quad \mathbf{a}_{3/4} = [0, 0, 1, \pm 1]. \qquad (26b)$$

They consist of relative ($-$) and collective ($+$) modes. Intuitive arguments allow a comparison of the respective relaxation rates. For example, when the spheres translate in opposite directions (relative translational mode $\mathbf{a}_2$), some fluid has to be pulled into or squeezed out of the region between the two particles; or when they rotate in opposite directions (relative rotational mode $\mathbf{a}_4$), the fluid between the spheres has to be sheared. On the other hand, when the spheres translate or rotate collectively (modes $\mathbf{a}_1$ or $\mathbf{a}_3$), the fluid surrounding the spheres is just "displaced" or "rotated" as a whole. So the collective modes experience less resistance

and therefore relax faster than the relative modes. This is in accordance with Eqs. (26) which give $\lambda_1 > \lambda_2$ and $\lambda_3 > \lambda_4$.

B. Transversal eigenmodes

The appropriate coordinates to treat the transversal eigenmodes are $\mathbf{q} = [r_{1x}, r_{2x}, \chi_{1y}, \chi_{2y}]$, and the mobility matrix $\mathbf{m}$ is given by Eq. (10). The polarization of the traps has to be chosen along the x or z direction so that the angles χ_{iy} are small.

The diagonalization of the nonsymmetric 4×4 matrix $\mathbf{mk}$ is not immediately obvious. However, symmetry arguments help to identify the eigenvectors. Since the two particles are identical and since spatial coordinates and angles possess different parities, one readily shows that the eigenvectors have to be of the form $[A, A, B, -B]$ or $[A, -A, B, B]$. This constraint simplifies the determination of the eigenmodes considerably. There are two relaxational modes with symmetric translation and antisymmetric rotation,

$$\lambda_{1/2} = \tfrac{1}{2}[k^t \mu_+^{tt\perp} + k^r \mu_-^{rr\perp} \pm \sqrt{(k^t \mu_+^{tt\perp} - k^r \mu_-^{rr\perp})^2 + 4k^t k^r (\mu_-^{tr\perp})^2}],$$
(27a)

$$\mathbf{a}_{1/2} = [A_{1/2}, A_{1/2}, B_{1/2}, -B_{1/2}],$$
(27b)

where

$$A_{1/2} = -2k^r \mu_-^{tr\perp},$$
(27c)

$$B_{1/2} = -(k^t \mu_+^{tt\perp} - k^r \mu_{-rr\perp}$$
$$\pm \sqrt{(k^t \mu_+^{tt\perp} - k^r \mu_-^{rr\perp})^2 + 4k^t k^r (\mu_-^{tr\perp})^2},$$
(27d)

and two modes with antisymmetric translation and symmetric rotation,

$$\lambda_{3/4} = \tfrac{1}{2}[k^t \mu_-^{tt\perp} + k^r \mu_+^{rr\perp} \pm \sqrt{(k^t \mu_-^{tt\perp} - k^r \mu_+^{rr\perp})^2 + 4k^t k^r (\mu_+^{tr\perp})^2}],$$
(28a)

$$\mathbf{a}_{3/4} = [A_{3/4}, -A_{3/4}, B_{3/4}, B_{3/4}],$$
(28b)

where

$$A_{3/4} = -2k^r \mu_+^{tr\perp},$$
(28c)

$$B_{3/4} = -(k^t \mu_-^{tt\perp} - k^r \mu_+^{rr\perp})$$
$$\pm \sqrt{(k^t \mu_-^{tt\perp} - k^r \mu_+^{rr\perp})^2 + 4k^t k^r (\mu_+^{tr\perp})^2}.$$
(28d)

Here, we use the abbreviations $\mu_\pm^{tt\perp} = \mu_{11}^{tt\perp} \pm \mu_{12}^{tt\perp}$, etc.

Without relying on the exact values of all the mobilities, we can already infer the qualitative characteristics of the eigenmodes based on general arguments. The signs of the components B_{1-4} are independent of the mobility coefficients. It is $B_1 > 0$, $B_2 < 0$, $B_3 > 0$, and $B_4 < 0$. The signs of A_{1-4} depend on the signs of $\mu_\pm^{tr\perp}$. In Sec. II C, we already discussed on the basis of the reflection method that the absolute value of the cross mobility $\mu_{12}^{tr\perp}$ is larger than the self-mobility $\mu_{11}^{tr\perp}$. Furthermore, by considering the special
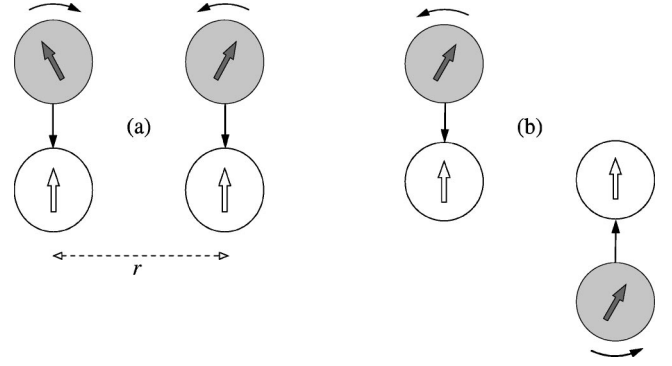

FIG. 4. Transversal eigenmodes of two trapped spheres (white: relaxed equilibrium state). There are two modes with collective translation and relative rotation (a) and two modes with relative translation and collective rotation (b). For each mode shown, there is a complementary mode with opposite direction of rotation.

case $v_{1x} = -\mu_{12}^{tr\perp} T_{2y}$ (for the geometry, see Fig. 2), we infer that $\mu_{12}^{tr\perp}$ is positive. Thus, $\mu_+^{tr\perp} > 0$ and $\mu_-^{tr\perp} < 0$, and we find $A_{1/2} > 0$ and $A_{3/4} < 0$.

We note that all eigenvalues of $\mathbf{mk}$ are positive. To prove this statement, we require $\lambda_n > 0$ in Eqs. (27a) and (28a) and find the condition $\mu_\pm^{tt\perp} \mu_\mp^{rr\perp} > (\mu_\mp^{tr\perp})^2$, which is the same guaranteeing that the mobility matrix is positive definite.

The eigenmodes described by Eqs. (27b) and (28b) are illustrated in Fig. 4. The mode in Fig. 4(a) corresponds to the eigenvector $\mathbf{a}_1$, and the one in Fig. 4(b) to $\mathbf{a}_3$. Each of the modes is complemented by a mode with opposite direction of rotation corresponding to the eigenvectors $\mathbf{a}_2$ and $\mathbf{a}_4$, respectively. Figure 4 shows the faster modes, i.e., $\lambda_1 > \lambda_2$ and $\lambda_3 > \lambda_4$. The reason for this is simply that the relaxations described by $\mathbf{a}_1$ and $\mathbf{a}_3$ show qualitatively the same behavior as if the particles were not trapped with respect to their orientations ($k^r = 0$). Hence, $\mathbf{a}_2$ and $\mathbf{a}_4$ correspond to modes where the orientational relaxation is opposite to this "natural" direction of rotation. Therefore, these modes are slower compared to their respective partners $\mathbf{a}_1$ and $\mathbf{a}_3$.

These qualitative considerations are in agreement with exact numbers for the eigenvalues which we plot in Fig. 5 as a function of the particle distance. Furthermore, for large distances, rotational and transversal motions decouple since $\lambda_{1/3}$ tend towards the single-particle translational relaxation rate $k^t \mu^t$ whereas $\lambda_{2/4}$ assume the corresponding rotational value $k^r \mu^r$. As obvious from the figure, this decoupling occurs for the rotational motion at shorter distances compared to translations since rotational flow fields decay faster than translational ones.

IV. TIME CORRELATIONS IN BROWNIAN MOTION

To treat the Brownian motion of the two spheres, time-dependent random forces and torques $\tilde{\mathbf{f}}(t)$ mimicking the microscopic degrees of freedom of the surrounding fluid have to be added. The total generalized force vector is then $\mathbf{f} = -\mathbf{kq} + \tilde{\mathbf{f}}(t)$. Extending Eq. (24), we obtain the Langevin-type equation
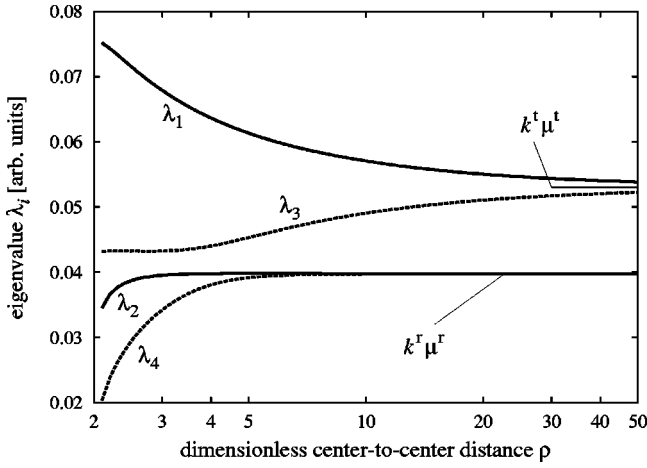
FIG. 5. Eigenvalues of the transversal modes [Eqs. (27a) and (28a)] as a function of the dimensionless center-to-center distance $\rho = r/a$. The mobilities were calculated using the numerical library HYDROLIB [28]. The trap constants are chosen as $k^{\mathrm{t}} = k^{\mathrm{r}}$.

$$\dot{\mathbf{q}} + \mathbf{mk}\mathbf{q} = \mathbf{m}\widetilde{\mathbf{f}}(t), \tag{29}$$

which describes a so-called Ornstein-Uhlenbeck process [32]. The random force is assumed to be a Gaussian white noise and is fully characterized by its first and second moments,

$$\langle \widetilde{\mathbf{f}}(t) \rangle = \mathbf{0}, \quad \langle \widetilde{\mathbf{f}}(t) \otimes \widetilde{\mathbf{f}}(t') \rangle = 2k_{\mathrm{B}}T\,\mathbf{m}^{-1}\delta(t-t'). \tag{30}$$

The fluctuation-dissipation theorem (30) relates the second moment of the fluctuating forces and torques to the friction matrix $\mathbf{m}^{-1}$ [33].

The formal solution of the Ornstein-Uhlenbeck process described by Eq. (29) reads [32]

$$\mathbf{q}(t) = e^{-\mathbf{mk}t}\mathbf{q}(0) + \int_0^t dt'\, e^{-\mathbf{mk}(t-t')}\mathbf{m}\widetilde{\mathbf{f}}(t'), \tag{31}$$

where the matrix exponential is defined, as usual, by its Taylor expansion $e^{-\mathbf{mk}t} = \sum_{s=0}^{\infty}(-\mathbf{mk}t)^s/s!$ Since we are only interested in the fluctuating part of $\mathbf{q}(t)$, we omit the deterministic relaxation $e^{-\mathbf{mk}t}\mathbf{q}(0)$ due to an initial displacement by choosing $\mathbf{q}(0) = \mathbf{0}$. In calculating the correlation matrix, we employ the second part of Eq. (30) and consider the long-time limit $(t \gg \lambda_n^{-1})$, where the system has relaxed to thermal equilibrium. We finally obtain

$$\langle \mathbf{q}(t+\tau) \otimes \mathbf{q}(t) \rangle = k_{\mathrm{B}}T e^{-\mathbf{mk}\tau}\mathbf{k}^{-1}, \quad \tau \geq 0. \tag{32}$$

Note that the correlation matrix is symmetric, i.e., $\langle \mathbf{q}(t_1) \otimes \mathbf{q}(t_2) \rangle = \langle \mathbf{q}(t_2) \otimes \mathbf{q}(t_1) \rangle$.

To express the correlation functions explicitly in coordinates, we introduce the dual eigenvectors $\mathbf{b}_n$ via $(\mathbf{mk})^{\mathrm{T}}\mathbf{b}_n = \lambda_n\mathbf{b}_n$. Together with the eigenvectors $\mathbf{a}_n$, they fulfill the orthonormality and completeness relations: $\mathbf{a}_m \cdot \mathbf{b}_n = \delta_{mn}$ and $\sum_n \mathbf{a}_n \otimes \mathbf{b}_n = \mathbf{1}$. Representing the matrix exponential by its spectral decomposition, $e^{-\mathbf{mk}t} = \sum_n e^{-\lambda_n t}\mathbf{a}_n \otimes \mathbf{b}_n$, we obtain from Eq. (32)
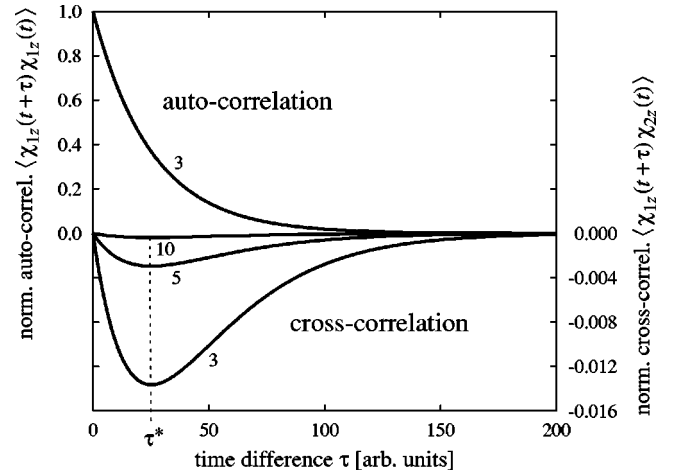

FIG. 6. Correlation functions for longitudinal rotational motions. The curve labels indicate the dimensionless center-to-center distance $\rho = r/a$. The functions are normalized to the mean square angular displacement $\langle \chi_{iz}^2 \rangle = k_{\mathrm{B}}T/k^{\mathrm{r}}$. The mobilities were calculated using the numerical library HYDROLIB [28].

$$\langle q_m(t+\tau)q_n(t) \rangle = \frac{k_{\mathrm{B}}T}{k_{nn}}\sum_l e^{-\lambda_l\tau}a_{lm}b_{ln}, \tag{33}$$

where a_{lm} (b_{ln}) is the mth (nth) component of the vector $\mathbf{a}_l$ ($\mathbf{b}_l$) and k_{nn} the nth element of the diagonal matrix $\mathbf{k}$ ($k_{nn} = k^{\mathrm{t}}, k^{\mathrm{t}}, k^{\mathrm{r}}, k^{\mathrm{r}}$). Normalizing the correlation function to the square roots of the mean square displacements $\langle q_n^2 \rangle = k_{\mathrm{B}}T/k_{nn}$, we finally arrive at

$$\frac{\langle q_m(t+\tau)q_n(t) \rangle}{\sqrt{\langle q_m^2 \rangle \langle q_n^2 \rangle}} = \sqrt{\frac{k_{mm}}{k_{nn}}}\sum_l e^{-\lambda_l\tau}a_{lm}b_{ln}. \tag{34}$$

A. Longitudinal motions

Longitudinal motions are characterized by the eigenvectors and eigenvalues in Eq. (26). Translations and rotations are decoupled. So the respective autocorrelations ($+$) and cross-correlation ($-$) for rotational motions are given by $[\exp(-k^{\mathrm{r}}\mu_+^{\mathrm{rr}\|}\tau) \pm \exp(-k^{\mathrm{r}}\mu_-^{\mathrm{rr}\|}\tau)]/2$, where $\mu_\pm^{\mathrm{rr}\|} = \mu_{11}^{\mathrm{rr}\|} \pm \mu_{12}^{\mathrm{rr}\|}$. For translations, the correlation functions are the same, however the relaxation rates are replaced by $k^{\mathrm{t}}\mu_\pm^{\mathrm{tt}\|}$ [18–20].

The correlations for translational motions have already been measured experimentally and compared with theoretical predictions [18–20]. These works reveal a good agreement between theory and experiment. The correlation functions for rotational motions show the same qualitative behavior (Fig. 6), however with some quantitative differences.

First of all, we realize that the strength of the cross-correlations decreases with increasing particle separation. This is explained by the decrease of the cross mobility $\mu_{12}^{\mathrm{rr}\|}$, which is due to the spatial decay of the flow fields created by the particle rotation. Compared to translational motions, this decrease is more pronounced since rotational flow fields decay stronger than their translational counterparts.

Second, while the autocorrelation reveals the typical monotonous decay, the cross-correlation function features an interesting behavior. It is negative (denoted as "anticorrelation" in Ref. [18]), since the relative modes decay more slowly than the collective ones, as already mentioned in Sec. III A. Therefore, the negative term in the cross-correlation function in the first paragraph dominates.

The most interesting feature of the cross-correlation function is that it exhibits a "memory effect." It vanishes at $\tau = 0$, in contrast to what one would initially expect for the instantaneous hydrodynamic forces in Stokesian dynamics, and then shows a distinct time-delayed extremum (located at τ^* in Fig. 6). This behavior can be understood as follows. The motion of particle 1 creates a fluid flow which instantaneously reaches particle 2. However, due to the trap, particle 2 can only "react" in a finite time. Thus, the correlation evolves on a characteristic time scale which is related to the relaxation times and thereby to the trap stiffness. Since the "memory" is "stored" in the trap, it cannot last longer than the typical relaxation time. Hence, the correlation decays to zero for times larger than τ^*.

For sufficiently large particle distances, the self-mobility $\mu_{11}^{\mathrm{rr}\|}$ is much bigger than the cross mobility $\mu_{12}^{\mathrm{rr}\|}$. Then, to leading order, the characteristic time scale is given by the single-particle rotational relaxation time $\tau^* = (k^{\mathrm{r}}\mu^{\mathrm{r}})^{-1}$, in analogy to the translational case [18–20]. Indeed, according to Fig. 6, τ^* depends only very weakly on the particle distance. Nevertheless, the cross mobility $\mu_{12}^{\mathrm{rr}\|}$ is sufficiently large to separate the two time scales $(k^{\mathrm{r}}\mu_{+}^{\mathrm{rr}\|})^{-1}$ and $(k^{\mathrm{r}}\mu_{-}^{\mathrm{rr}\|})^{-1}$, which is the origin of the anticorrelation.

B. Transversal motions

The transversal eigenmodes are characterized by Eqs. (27) and (28). Since the two types of eigenvectors are orthogonal to each other, i.e., $\mathbf{a}_{1/2} \cdot \mathbf{a}_{3/4} = 0$, the dual vectors $\mathbf{b}_{1/2}$ are linear combinations of $\mathbf{a}_1$ and $\mathbf{a}_2$ only; the equivalent holds for $\mathbf{b}_{3/4}$. One finds

$$\mathbf{b}_n = \frac{|\mathbf{a}_{\bar{n}}|^2 \mathbf{a}_n - (\mathbf{a}_n \cdot \mathbf{a}_{\bar{n}})\mathbf{a}_{\bar{n}}}{|\mathbf{a}_n|^2|\mathbf{a}_{\bar{n}}|^2 - (\mathbf{a}_n \cdot \mathbf{a}_{\bar{n}})^2}, \qquad (35)$$

where the index combinations are $(n|\bar{n}) = (1|2)$, $(2|1)$, $(3|4)$, $(4|3)$. The correlation functions for the coordinates $q_1 = r_{1x}$, $q_2 = r_{2x}$, $q_3 = \chi_{1y}$, and $q_4 = \chi_{2y}$ are obtained from Eq. (34). Now, they are linear combinations of four exponential decays.

The autocorrelation functions $\langle r_{1x}(t+\tau)r_{1x}(t)\rangle$ and $\langle \chi_{1y}(t+\tau)\chi_{1y}(t)\rangle$ show qualitatively the same monotonous decay as in the case of longitudinal fluctuations (see Fig. 6). All the other correlation functions exhibit the features of the longitudinal cross correlation discussed in Sec. IV A (except for the sign).

As representative examples, the correlation functions for rotations about the y axis and translations along the x direction, $\langle \chi_{1y}(t+\tau)r_{1x}(t)\rangle$ and $\langle \chi_{1y}(t+\tau)r_{2x}(t)\rangle$, are plotted in Fig. 7. In the following, we will refer to them briefly as mixed self-correlation and cross correlation, describing the
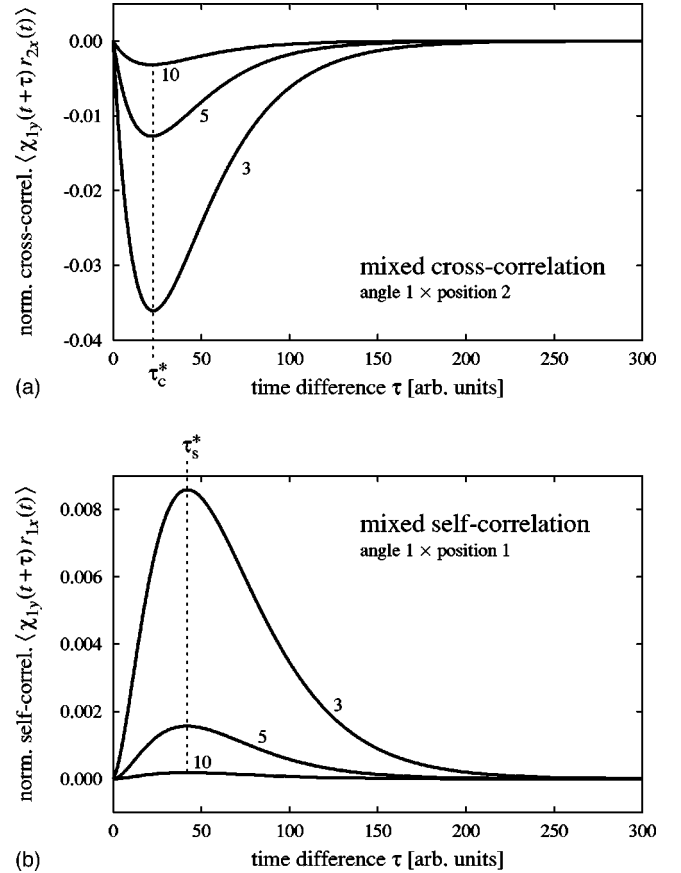

FIG. 7. Correlation functions for transversal motions. The curves shown are the mixed cross-correlation and self-correlation for angle and position. The curve labels indicate the dimensionless center-to-center distance $\rho = r/a$. The trap constants are chosen as $k^{\mathrm{t}} = k^{\mathrm{r}}$. The functions are normalized to the square roots of the mean square displacements $\langle \chi_{iy}^2 \rangle = k_{\mathrm{B}}T/k^{\mathrm{r}}$ and $\langle r_{ix}^2 \rangle = k_{\mathrm{B}}T/k^{\mathrm{t}}$ [see Eq. (34)].

self-coupling and cross coupling of rotation and translation, respectively.

Both correlation functions show a distinct time-delayed extremum, denoted by τ_s^* and τ_c^* in Fig. 7. The mixed cross correlation is interpreted in the same fashion as the longitudinal cross correlation in the preceding section.

The most striking feature is revealed by the mixed self-correlation. For a single sphere, translation and rotation are not coupled [31], i.e., the mixed (self-)correlation vanishes. However, in the two-sphere system, there exists a mixed self-correlation, as shown in Fig. 7, that is mediated by the neighboring particle. This correlation is weaker than the mixed cross correlation since the flow field created by particle 1 has to be reflected by particle 2. As discussed before, particle 2 reacts with a finite delay due to the trap stiffness. Then, in addition, particle 1 also has a finite "reaction time." Hence, we always expect $\tau_s^* > \tau_c^*$.

We also studied the influence of the trap stiffnesses k^{t} and k^{r} on the correlation functions. As illustrated in Fig. 8, the difference in the delay times τ_s^* and τ_c^* decreases with increasing ratio $k^{\mathrm{t}}/k^{\mathrm{r}}$. Furthermore, we observe that the correlations are strongest for $k^{\mathrm{t}} \approx k^{\mathrm{r}}$.
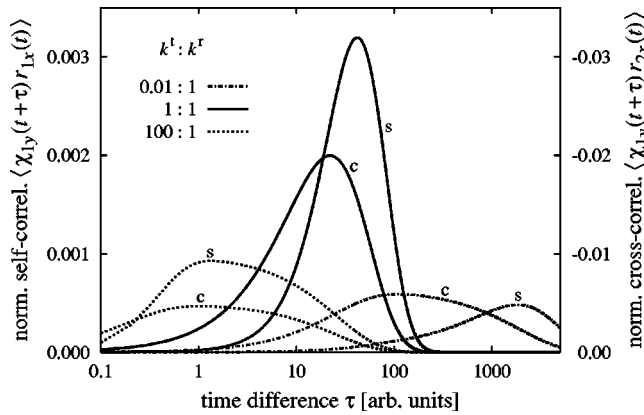
FIG. 8. Mixed self-correlation (label s) and cross correlation (label c) for various trap constant ratios k^t:k^r. The force constant k^t was varied ($k^t = 0.01$, 1, and 100), while the torque constant was kept fixed ($k^r = 1$). The qualitative behavior of the functions (discussion see text) is the same for different particle distances (here $\rho = 4$).

Note that the mixed self-correlations cannot be treated within the Rotne-Prager approximation. They constitute an additional effect of higher order, as mentioned in Sec. II C.

V. CONCLUSIONS

In this paper, we have presented the complete solution for the hydrodynamically coupled translational and rotational motions of two colloidal spheres that are harmonically trapped with respect to both their positions and orientations.

Based on pure symmetry arguments and without relying on explicit values of the mobilities, we have determined all the 12 collective eigenmodes and qualitatively discussed their relaxation times. Whereas the properties of the longitudinal modes are reminiscent to a system with pure translational degrees of freedom, the transversal modes exhibit a characteristic coupling of translation and rotation.

In a detailed Langevin-type analysis, we have been able to derive the full set of correlation functions characterizing the Brownian motion of the particles in the optical traps. The analysis relies on the eigenvalue problem of nonsymmetric matrices. Explicit examples for the correlation functions at different particle separations have been calculated based on mobilities which we obtained from the numerical library HYDROLIB [28].

The longitudinal fluctuations exhibit the features already mentioned in Refs. [18–20], namely, a memory effect in the cross correlations. The transverals fluctuations are governed by the coupling of translations and rotations. As the most striking feature, this coupling is also visible in the self-correlations which are governed by a second delay time in addition to the one observed in the cross correlations. The self-coupling of translation and rotation for one sphere has to be mediated by a second sphere. It is not included in the Rotne-Prager approximation and therefore introduces an additional effect of higher order.

Correlation functions involving the rotational degrees of freedom are weaker compared to pure translational correlations since the flow field of a single rotating sphere decays as $1/r^2$, compared to translating particles where the decay is $1/r$. However, the strength of the correlations increases for decreasing particle separation which is more pronounced whenever rotations are involved. Furthermore, at sufficiently small distances, lubrication theory becomes important [34], and the system introduced in this paper may help to check its predictions.

Our work stresses the rotational degree of freedom and its influence on hydrodynamic interactions. We hope to stimulate experimental investigations of the correlation functions presented in this paper.

In the Introduction, we have already mentioned the field of microrheology. An extension of our work to viscoelastic media based on the theoretical approach presented in Ref. [17] seems appealing. The rotational motion of the probe particle results in an interesting deformational mode since it introduces some torsion in the surrounding medium. It therefore can yield additional information about the viscoelastic properties.

[1] P. N. Pusey, in *Liquids, Freezing, and Glass Transition*, Proceedings of the Les Houches Summer School of Theoretical Physics 1989, Part II, edited by J. P. Hansen, D. Levesque, and J. Zinn-Justin (North-Holland, Amsterdam, 1991), p. 763.

[2] W. Poon, P. Pusey, and H. Lekkerkerker, Phys. World **4**, 27 (1996).

[3] J. K. G. Dhont, *An Introduction to Dynamics of Colloids* (Elsevier, Amsterdam, 1996).

[4] J. Happel and H. Brenner, *Low Reynolds Number Hydrodynamics* (Noordhoff, Leiden, 1973).

[5] B.U. Felderhof, Physica A **151**, 1 (1988).

[6] H. Brenner, Chem. Eng. Sci. **18**, 1 (1963); **19**, 599 (1964).

[7] R.B. Jones, Physica A **150**, 339 (1988); **157**, 752 (1989).

[8] V. Degiorgio, R. Piazza, and R.B. Jones, Phys. Rev. E **52**, 2707 (1995).

[9] G.H. Koenderink, H. Zhang, M.P. Lettinga, G. Nägele, and A.P. Philipse, Phys. Rev. E **64**, 022401 (2001).

[10] A.J.C. Ladd, Phys. Fluids A **5**, 299 (1993).

[11] M.P. Brenner, Phys. Fluids A **11**, 754 (1999).

[12] T.M. Squires and M.P. Brenner, Phys. Rev. Lett. **85**, 4976 (2000).

[13] T.G. Mason, K. Ganesan, J.H. van Zanten, D. Wirtz, and S.C. Kuo, Phys. Rev. Lett. **79**, 3282 (1997).

[14] F. Gittes, B. Schnurr, P.D. Olmsted, F.C. MacKintosh, and C.F.

Schmidt, Phys. Rev. Lett. **79**, 3286 (1997).

[15] F.G. Schmidt, B. Hinner, and E. Sackmann, Phys. Rev. E **61**, 5646 (2000).

[16] J.C. Crocker, M.T. Valentine, E.R. Weeks, T. Gisler, P.D. Kaplan, A.G. Yodh, and D.A. Weitz, Phys. Rev. Lett. **85**, 888 (2000).

[17] A.J. Levine and T.C. Lubensky, Phys. Rev. Lett. **85**, 1774 (2000); Phys. Rev. E **65**, 011501 (2001).

[18] J.-C. Meiners and S.R. Quake, Phys. Rev. Lett. **82**, 2211 (1999).

[19] P. Bartlett, S.I. Henderson, and S.J. Mitchell, Philos. Trans. R. Soc. London, Ser. A **359**, 883 (2001).

[20] S. Henderson, S. Mitchell, and P. Bartlett, Phys. Rev. E **64**, 061403 (2001).

[21] L. Starrs and P. Bartlett, J. Phys.: Condens. Matter **15**, S251 (2003).

[22] J.C. Crocker, J. Chem. Phys. **106**, 2837 (1997).

[23] E.R. Dufresne, T.M. Squires, M.P. Brenner, and D.G. Grier, Phys. Rev. Lett. **85**, 3317 (2000).

[24] D.R. Cairns, M. Sibulkin, and G.P. Crawford, Appl. Phys. Lett. **78**, 2643 (2001).

[25] A. Mertelj, J.L. Arauz Lara, G. Maret, T. Gisler, and H. Stark, Europhys. Lett. **59**, 337 (2002).

[26] S. Juodkazis, M. Shikata, T. Takahashi, S. Matsuo, and H. Misawa, Appl. Phys. Lett. **74**, 3627 (1999).

[27] B. Cichocki, B.U. Felderhof, K. Hinsen, E. Wajnryb, and J. Bławdziewicz, J. Chem. Phys. **100**, 3780 (1994).

[28] K. Hinsen, Comput. Phys. Commun. **88**, 327 (1995).

[29] D.J. Jeffrey and Y. Onishi, J. Fluid Mech. **139**, 261 (1984).

[30] P. Mazur and W. van Saarloos, Physica A **115**, 21 (1982).

[31] S. Hess, Z. Naturforsch. A **23A**, 1095 (1968).

[32] H. Risken, *The Fokker-Planck Equation* (Springer, Berlin, 1989).

[33] E.H. Hauge and A. Martin-Löf, J. Stat. Phys. **7**, 259 (1973).

[34] S. Kim and R.T. Mifflin, Phys. Fluids **28**, 2033 (1985).